



Article

Fractional View Analysis of Cahn–Allen Equations by New Iterative Transform Method

Liaquat Ali ¹, Rasool Shah ² and Wajaree Weera ^{3,*} ¹ School of Sciences, Xi'an Technological University, Xi'an 710021, China; liaquat@xatu.edu.cn² Department of Mathematics, Abdul Wali Khan University of Mardan, Mardan 23200, Pakistan; rasoolshahawkum@gmail.com³ Department of Mathematics, Faculty of Science, Khon Kaen University, Khon Kaen 40002, Thailand

* Correspondence: wajawe@kku.ac.th

Abstract: In this article, the new iterative transform method is applied to evaluate the time-fractional Cahn–Allen model solution. In this technique, Elzaki transformation is a mixture of the new iteration technique. Two problems are studied to demonstrate and confirm the accuracy of the proposed technique. The current technique's mathematical analysis showed that the method is simple to understand and reliable. These solutions indicate that the proposed technique is advantageous and simple to apply in science and engineering problems.

Keywords: Elzaki transform; new iterative method; Caputo derivatives; Cahn–Allen equation



Citation: Ali, L.; Shah, R.; Weera, W. Fractional View Analysis of Cahn–Allen Equations by New Iterative Transform Method. *Fractal Fract.* **2022**, *6*, 293. <https://doi.org/10.3390/fractalfract6060293>

Academic Editor: Haci Mehmet Baskonus

Received: 5 May 2022

Accepted: 26 May 2022

Published: 27 May 2022

Publisher's Note: MDPI stays neutral with regard to jurisdictional claims in published maps and institutional affiliations.



Copyright: © 2022 by the authors. Licensee MDPI, Basel, Switzerland. This article is an open access article distributed under the terms and conditions of the Creative Commons Attribution (CC BY) license (<https://creativecommons.org/licenses/by/4.0/>).

1. Introduction

The subject of fractional calculus (FC) is part of modern calculus where the fractional-order derivative of the function can be used to calculate various long time dynamics and other useful information of the targeted phenomena. The applications of fractional calculus are observed in numerous disciplines such as manipulating ideas of dynamical systems, electrical community optics and signal processing can be effectively modeled by means of linear or nonlinear fractional differential equations (FDEs).

The investigation of fractional order integrals and derivatives is an interesting study of fractional calculus. It has increased the broad consideration of scientists in the last two centuries. It has uncommon implementations in differing areas of engineering and medical science. In this specific situation, Riemann and Liouville were the pioneers who gave the ideas of fractional derivatives and integrals [1]. From these definitions, scientists began to think and characterized fractional equations, which are expansions and speculations of Riemann–Liouville ideas. Over time, many new interesting models have been formulated in the field of fractional calculus [2,3]. For instance, Caputo gave an improved formula in the area of fractional calculus.

Nonlinear partial differential equations play a significant and upgraded role in demonstrating various physical appearances identified with fluid mechanics, plasma physics, solid-state physics, population dynamics, chemical kinetics, nonlinear optics, soliton theory, protein chemistry, etc. These nonlinear models, like their scientific arrangements, arouse a lot of interest in appropriate disciplines. Nonlinear models play a crucial role in a variety of phenomena in many of the domains of applied science listed above [4–7].

The fractional partial differential equations (FPDEs) are the most suitable class of FDEs to model various complex phenomena of applied sciences. The important models represented by FPDEs include ground water float and El Niño–Southern oscillation mannequin. The improved mathematical models of FPDEs are of much importance to analyze natural processes. Therefore, researchers have attempted to solve these models numerically or analytically to explore the correct dynamics of the suggested phenomena [8,9].

Being influenced by ongoing research in this area, we find out about the fractional order Cahn–Allen equation (FCA), which is a very necessary mathematical model written as follows:

$$D_{\eta}^{\alpha} \phi(\varepsilon, \eta) - \phi_{rr}(\varepsilon, \eta) + \phi^3(\varepsilon, \eta) - \phi(\varepsilon, \eta) = 0, \quad \varepsilon > 0, \quad 0 < \rho \leq 1, \quad \phi(\varepsilon, 0) = f(\varepsilon). \quad (1)$$

In exceptional cases when $\alpha = 1$, the fractional order Cahn–Allen equation is changed into the classical Cahn–Allen equation. Esen et al. [10] utilized the homotopy analysis method to accumulate the fractional order analytical solution of Cahn–Allen equation. The time-fractional Cahn–Allen equation was studied in [11] by the fractional sub-equation method for finding an approximate solution of the S-H equation. The (G'/G) -expansion method was used by Yasar et al. for finding a series solution of the spacetime Cahn–Allen equation in [12]. The Haar wavelet method [13] was utilized by Hariharan et al. to find a numerical solution of the Cahn–Allen equation. Solitary and periodic wave solutions for the Cahn–Allen equation were found by Tascan et al. in [14]. The modified handy equation technique is applied to gain new actual choices of the Cahn–Allen equation and the received consequences are moreover in agreement with Tascan et al.'s penalties [15]. The double exp-function method was applied by Bekir et al. [16] to the Cahn–Allen equation for finding one-soliton and two-soliton solutions. Three techniques are studied for the time-fractional order Cahn–Allen equation by Gner et al. in [17].

Daftardar-Gejji and Jafari introduced a new iterative method of analysis for analysis of nonlinear equations in 2006 [18,19]. The first application of Laplace transformation in an iterative technique was presented by Jafari et al. The iterative Laplace transformation method [20] was introduced as a simple method for estimating the approximate effective of the fractional partial differential equation scheme. The new iterative transform method (NITM) was implemented to solve linear and nonlinear partial differential equations such as fractional-order Fornberg Whitham equations [21], the time-fractional Zakharov Kuznetsov equation [22], and fractional-order Fokker–Planck equations [23].

The NITM is applied to investigate fractional-order Cahn–Allen equations. The solution of the problem is discuss regarding the accuracy of the current technique. The outcomes of the fractional-order equations as well as integral-order equations are determined by applying the current technique. Other linear and nonlinear fractional-order partial differential equations can also benefit from the same technique.

The rest of the paper is organized as follows. In Section 2, the important preliminaries are discussed, the NITM procedure is presented in Section 3 and the generalized concept of the NITM is given in Section 5. In Section 4, the numerical implementation of the NITM is described and the higher accuracy of the NITM and closed contact with actual solutions of the targeted problems are confirmed.

2. Basic Concepts

Definition 1. The Riemann–Liouville fractional operator D^{γ} of order γ is defined as [24–26]

$$D^{\gamma} v(\varepsilon) = \begin{cases} \frac{d^m}{d\varepsilon^m} v(\varepsilon), & \gamma = m; \\ \frac{1}{\Gamma(m-\gamma)} \frac{d}{d\varepsilon^m} \int_0^{\varepsilon} \frac{v(\psi)}{(\varepsilon-\psi)^{\gamma-m+1}} d\psi, & m-1 < \gamma < m, \end{cases}$$

where $m \in \mathbb{Z}^+$, $\gamma \in \mathbb{R}^+$ and

$$D^{-\gamma} v(\varepsilon) = \frac{1}{\Gamma(\gamma)} \int_0^{\varepsilon} (\varepsilon - \psi)^{\gamma-1} v(\psi) d\psi, \quad 0 < \gamma \leq 1.$$

Definition 2. The fractional Riemann–Liouville integral operator M^{ψ} is defined as [24–26]

$$J^{\gamma} v(\varepsilon) = \frac{1}{\Gamma(\gamma)} \int_0^{\varepsilon} (\varepsilon - \psi)^{\gamma-1} v(\psi) d\psi, \quad \varepsilon > 0, \quad \gamma > 0.$$

The operator of basic properties:

$$J^\gamma \varepsilon^m = \frac{\Gamma(m+1)}{\Gamma(m+\gamma+1)} \varepsilon^{m+\gamma},$$

$$D^\gamma \varepsilon^m = \frac{\Gamma(m+1)}{\Gamma(m-\gamma+1)} \varepsilon^{m-\gamma}.$$

Definition 3. The Caputo fractional operator D^γ of γ is defined as [24–26]

$${}^C D^\gamma \nu(\varepsilon) = \begin{cases} \frac{1}{\Gamma(m-\gamma)} \int_0^\varepsilon \frac{\nu^m(\psi)}{(\varepsilon-\psi)^{\gamma-m+1}} d\psi, & m-1 < \gamma < m; \\ \frac{d^m}{d\varepsilon^m} \nu(\varepsilon), & m = \gamma. \end{cases} \quad (2)$$

Definition 4.

$$J_\varepsilon^\gamma D_\varepsilon^\gamma g(\varepsilon) = g(\varepsilon) - \sum_{k=0}^m g^k(0^+) \frac{\varepsilon^k}{k!}, \quad \text{for } \varepsilon > 0, \text{ and } m-1 < \gamma \leq m, \quad m \in \mathbb{N}. \quad (3)$$

$$D_\varepsilon^\gamma J_\varepsilon^\gamma g(\varepsilon) = g(\varepsilon).$$

Definition 5. The fractional-order Caputo operator of Elzaki transformation is given as:

$$E[D_\varepsilon^\gamma g(\varepsilon)] = s^{-\gamma} E[g(\varepsilon)] - \sum_{k=0}^{m-1} s^{2-\gamma+k} g^{(k)}(0), \quad \text{where } m-1 < \gamma < m.$$

3. The General Discussion of the Technique

Consider the general form of FPDEs,

$$D_\eta^\rho \phi(\varepsilon, \eta) + M\phi(\varepsilon, \eta) + N\phi(\varepsilon, \eta) = h(\varepsilon, \eta), \quad m \in \mathbb{N}, \quad m-1 < \rho \leq m, \quad (4)$$

where M is linear and N nonlinear operators and the source term is h . With the initial condition

$$\phi^{(k)}(\varepsilon, 0) = g_k(\varepsilon), \quad k = 0, 1, 2, \dots, m-1, \quad (5)$$

we implement the Elzaki transformation of Equation (4) and we obtain

$$E[D_\eta^\rho \phi(\varepsilon, \eta)] + E[M\phi(\varepsilon, \eta) + N\phi(\varepsilon, \eta)] = E[h(\varepsilon, \eta)]. \quad (6)$$

Using the differentiation property of Elzaki transform is defined as

$$E[\phi(\varepsilon, \eta)] = \sum_{k=0}^m s^{2-\rho+k} \phi^{(k)}(\varepsilon, 0) + s^\rho E[h(\varepsilon, \eta)] - s^\rho E[M\phi(\varepsilon, \eta) + N\phi(\varepsilon, \eta)]. \quad (7)$$

The inverse Elzaki transformation converts Equation (7) into

$$\phi(\varepsilon, \eta) = E^{-1} \left[\left(\sum_{k=0}^m s^{2-\rho+k} \phi^{(k)}(\varepsilon, 0) + s^\rho E[h(\varepsilon, \eta)] \right) \right] - E^{-1} [s^\rho E[M\phi(\varepsilon, \eta) + N\phi(\varepsilon, \eta)]]. \quad (8)$$

Through an iterative technique, we have

$$\phi(\varepsilon, \eta) = \sum_{m=0}^{\infty} \phi_m(\varepsilon, \eta). \quad (9)$$

Further, the operator M is linear, therefore

$$M \left(\sum_{m=0}^{\infty} \phi_m(\varepsilon, \eta) \right) = \sum_{m=0}^{\infty} M[\phi_m(\varepsilon, \eta)], \quad (10)$$

and the operator N is nonlinear, therefore we have the following

$$N\left(\sum_{m=0}^{\infty} \phi_m(\varepsilon, \eta)\right) = \phi_0(\varepsilon, \eta) + N\left(\sum_{k=0}^m \phi_k(\varepsilon, \eta)\right) - M\left(\sum_{k=0}^m \phi_k(\varepsilon, \eta)\right). \quad (11)$$

Substituting Equations (9)–(11) in Equation (8), we obtain

$$\begin{aligned} \sum_{m=0}^{\infty} \phi_m(\varepsilon, \eta) = & E^{-1} \left[s^{\rho} \left(\sum_{k=0}^m s^{2-\varepsilon+k} \phi^k(\varepsilon, 0) + E[h(\varepsilon, \eta)] \right) \right] \\ & - E^{-1} \left[s^{\rho} E \left[M\left(\sum_{k=0}^m \phi_k(\varepsilon, \eta)\right) - N\left(\sum_{k=0}^m \phi_k(\varepsilon, \eta)\right) \right] \right]. \end{aligned} \quad (12)$$

Now, we apply the iterative method

$$\begin{aligned} \phi_0(\varepsilon, \eta) &= E^{-1} \left[s^{\rho} \left(\sum_{k=0}^m s^{2-\varepsilon+k} \phi^k(\varepsilon, 0) + s^{\rho} E(h(\varepsilon, \eta)) \right) \right], \\ \phi_1(\varepsilon, \eta) &= -E^{-1} [s^{\rho} E[M[\phi_0(\varepsilon, \eta)] + N[\phi_0(\varepsilon, \eta)]], \\ \phi_{m+1}(\varepsilon, \eta) &= -E^{-1} \left[s^{\rho} E \left[-M\left(\sum_{k=0}^m \phi_k(\varepsilon, \eta)\right) - N\left(\sum_{k=0}^m \phi_k(\varepsilon, \eta)\right) \right] \right], \quad m \geq 1. \end{aligned} \quad (13)$$

Finally, Equations (4) and (5) provide the m -term solution in series form, defined as

$$\phi(\varepsilon, \eta) \cong \phi_0(\varepsilon, \eta) + \phi_1(\varepsilon, \eta) + \phi_2(\varepsilon, \eta) + \cdots + \phi_m(\varepsilon, \eta), \quad m = 1, 2, \dots \quad (14)$$

4. Numerical Implementation

Example 1. Consider the time-fractional Cahn–Allen model given as

$$D_{\eta}^{\rho} \phi(\varepsilon, \eta) - \phi_{\varepsilon\varepsilon}(\varepsilon, \eta) + \phi^3(\varepsilon, \eta) - \phi(\varepsilon, \eta) = 0, \quad r > 0, \quad 0 < \rho \leq 1, \quad (15)$$

with initial conditions

$$\phi(\varepsilon, 0) = \frac{1}{1 + e^{-\frac{\varepsilon}{\sqrt{2}}}}. \quad (16)$$

The exact solution of the above equation, when $\rho = 1$, is

$$\phi(\varepsilon, \eta) = \frac{1}{1 + \left(e^{\frac{-\varepsilon}{\sqrt{2}} - \frac{3\eta}{2}} \right)}. \quad (17)$$

First, applying the Elzaki transform in Equation (15), we obtain

$$E[\phi(\varepsilon, \eta)] = s^2 \left(\frac{1}{1 + e^{-\frac{\varepsilon}{\sqrt{2}}}} \right) - s^{\rho} E[\phi_{\varepsilon\varepsilon}(\varepsilon, \eta) - \phi^3(\varepsilon, \eta) + \phi(\varepsilon, \eta)]. \quad (18)$$

Now, using the Elzaki inverse transformation, we obtain

$$\phi(\varepsilon, \eta) = \frac{1}{1 + e^{-\frac{\varepsilon}{\sqrt{2}}}} - E^{-1} [s^{\rho} E\{\phi_{\varepsilon\varepsilon}(\varepsilon, \eta) - \phi^3(\varepsilon, \eta) + \phi(\varepsilon, \eta)\}]. \quad (19)$$

Using the NITM, we have the following:

$$\begin{aligned}\phi_0(\varepsilon, \eta) &= \frac{1}{1 + e^{-\frac{\varepsilon}{\sqrt{2}}}}, \\ \phi_1(\varepsilon, \eta) &= -E^{-1}[s^\rho E\{\phi_{0\varepsilon\varepsilon}(\varepsilon, \eta) - \phi_0^3(\varepsilon, \eta) + \phi_0(\varepsilon, \eta)\}] = -\frac{3\eta^\rho}{4\rho \Gamma(\rho) + 4\rho \cosh\left(\frac{\varepsilon}{\sqrt{2}}\right)\Gamma(\rho)}, \\ \phi_2(\varepsilon, \eta) &= -E^{-1}[s^\rho E\{\phi_{1\varepsilon\varepsilon}(\varepsilon, \eta) - \phi_1^3(\varepsilon, \eta) + \phi_1(\varepsilon, \eta)\}] \\ \phi_2(\varepsilon, \eta) &= \frac{9}{256} \left(\frac{3\eta^\rho \left(-\frac{3\eta^\rho \Gamma(3\rho)}{(1 + \cosh^3(\frac{\varepsilon}{\sqrt{2}}))\Gamma(4\rho)} - \frac{64e^{\frac{3\varepsilon}{\sqrt{2}}}\Gamma(1+\rho)\Gamma(1+\rho)}{\left(1 + e^{\frac{\varepsilon}{\sqrt{2}}}\right)^5\Gamma(1+3\rho)} \right)}{\Gamma(1+3\rho)^3} - \frac{16\operatorname{sech}^2\left(\frac{\varepsilon}{2\sqrt{2}}\right)\tanh\left(\frac{\varepsilon}{2\sqrt{2}}\right)}{\Gamma(1+2\rho)} \right) \\ &\vdots\end{aligned}$$

The solution of the series form is given as

$$\phi(\varepsilon, \eta) = \phi_0(\varepsilon, \eta) + \phi_1(\varepsilon, \eta) + \phi_2(\varepsilon, \eta) + \phi_3(\varepsilon, \eta) + \cdots + \phi_n(\varepsilon, \eta). \quad (20)$$

The analytical result is obtained as

$$\begin{aligned}\phi(\varepsilon, \eta) &= \frac{1}{1 + e^{-\frac{\varepsilon}{\sqrt{2}}}} - \frac{3\eta^\rho}{4\rho \Gamma(\rho) + 4\rho \cosh\left(\frac{\varepsilon}{\sqrt{2}}\right)\Gamma(\rho)} \\ &+ \frac{9}{256} \left(\frac{3\eta^\rho \left(-\frac{3\eta^\rho \Gamma(3\rho)}{(1 + \cosh^3(\frac{\varepsilon}{\sqrt{2}}))\Gamma(4\rho)} - \frac{64e^{\frac{3\varepsilon}{\sqrt{2}}}\Gamma(1+\rho)\Gamma(1+\rho)}{\left(1 + e^{\frac{\varepsilon}{\sqrt{2}}}\right)^5\Gamma(1+3\rho)} \right)}{\Gamma(1+3\rho)^3} - \frac{16\operatorname{sech}^2\left(\frac{\varepsilon}{2\sqrt{2}}\right)\tanh\left(\frac{\varepsilon}{2\sqrt{2}}\right)}{\Gamma(1+2\rho)} \right) \dots \quad (21)\end{aligned}$$

Solution for $\rho = 1$

$$\begin{aligned}\phi(\varepsilon, \eta) &= \frac{1}{e^{-\frac{\varepsilon}{\sqrt{2}}} + 1} + \frac{3\eta}{4 \cosh\left(\frac{\varepsilon}{\sqrt{2}}\right) + 4} + \frac{9}{256} \eta^2 \left(3\eta \left(-\frac{\eta}{\left(\cosh\left(\frac{\varepsilon}{\sqrt{2}}\right) + 1\right)^3} - \frac{64e^{\frac{3\varepsilon}{\sqrt{2}}}}{3\left(e^{\frac{\varepsilon}{\sqrt{2}}} + 1\right)^5} \right) \right. \\ &\quad \left. - 8 \tanh\left(\frac{\varepsilon}{2\sqrt{2}}\right) \operatorname{sech}^2\left(\frac{\varepsilon}{2\sqrt{2}}\right) \right).\end{aligned}$$

Solution for $\rho = 0.95$

$$\begin{aligned}\phi(\varepsilon, \eta) &= \frac{1}{e^{-\frac{\varepsilon}{\sqrt{2}}} + 1} + \frac{3\eta^{0.95}}{3.91952 \cosh\left(\frac{\varepsilon}{\sqrt{2}}\right) + 3.91952} + \\ &\quad \frac{9}{256} \eta^{1.9} \left(3.18861 \eta^{0.95} \left(-\frac{1.11801 \eta^{0.95}}{\left(\cosh\left(\frac{\varepsilon}{\sqrt{2}}\right) + 1\right)^3} - \frac{22.9851 e^{\frac{3\varepsilon}{\sqrt{2}}}}{\left(e^{\frac{\varepsilon}{\sqrt{2}}} + 1\right)^5} \right) \right. \\ &\quad \left. - 8.75582 \tanh\left(\frac{\varepsilon}{2\sqrt{2}}\right) \operatorname{sech}^2\left(\frac{\varepsilon}{2\sqrt{2}}\right) \right).\end{aligned}$$

Solution for $\rho = 0.85$

$$\begin{aligned} \phi(\varepsilon, \eta) = & \frac{1}{e^{-\frac{\varepsilon}{\sqrt{2}}} + 1} + \frac{3\eta^{0.85}}{3.78244 \cosh\left(\frac{\varepsilon}{\sqrt{2}}\right) + 3.78244} + \\ & \frac{9}{256} \eta^{1.7} \left(3.548 \eta^{0.85} \left(-\frac{1.38643 \eta^{0.85}}{\left(\cosh\left(\frac{\varepsilon}{\sqrt{2}}\right) + 1\right)^3} - \frac{26.6087 e^{\frac{3\varepsilon}{\sqrt{2}}}}{\left(e^{\frac{\varepsilon}{\sqrt{2}}} + 1\right)^5} \right) \right. \\ & \left. - 10.3581 \tanh\left(\frac{\varepsilon}{2\sqrt{2}}\right) \operatorname{sech}^2\left(\frac{\varepsilon}{2\sqrt{2}}\right) \right). \end{aligned}$$

Solution for $\rho = 0.75$

$$\begin{aligned} \phi(\varepsilon, \eta) = & \frac{1}{e^{-\frac{\varepsilon}{\sqrt{2}}} + 1} + \frac{3\eta^{0.75}}{3.67625 \cosh\left(\frac{\varepsilon}{\sqrt{2}}\right) + 3.67625} + \\ & \frac{9}{256} \eta^{1.5} \left(3.86444 \eta^{0.75} \left(-\frac{1.6995 \eta^{0.75}}{\left(\cosh\left(\frac{\varepsilon}{\sqrt{2}}\right) + 1\right)^3} - \frac{30.6724 e^{\frac{3\varepsilon}{\sqrt{2}}}}{\left(e^{\frac{\varepsilon}{\sqrt{2}}} + 1\right)^5} \right) \right. \\ & \left. - 12.036 \tanh\left(\frac{\varepsilon}{2\sqrt{2}}\right) \operatorname{sech}^2\left(\frac{\varepsilon}{2\sqrt{2}}\right) \right). \end{aligned}$$

In Figures 1 and 2, we check how accurate this method is for solving the time-fractional Cahn–Allen equation. The approximation series solution acquired by the NITM is in very close agreement with the precise solution. In Figure 3, the 2D surface obtained by the NITM versus the exact solution is shown, while in Figure 4, the NITM solution of Example 1 is represented.

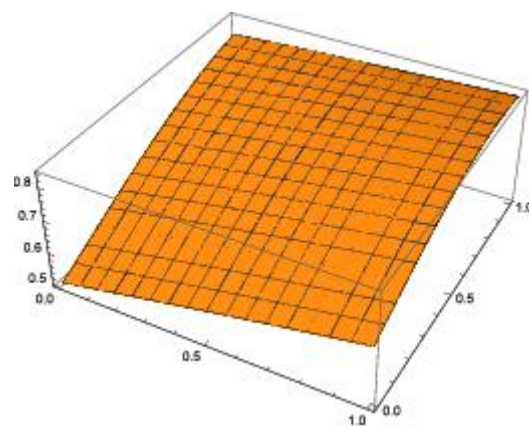


Figure 1. Approximate solution obtained by NITM for fractional-order Problem 1 when $\alpha = 1$.

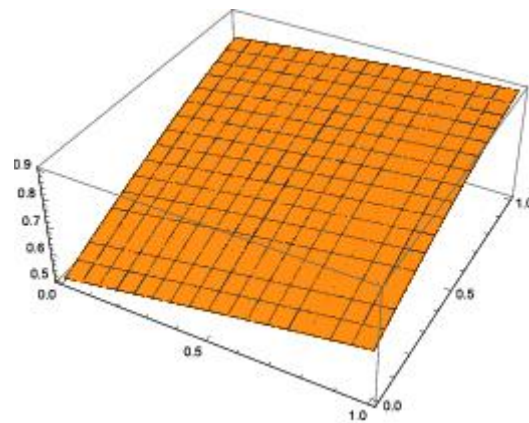


Figure 2. Exact solution graph of Problem 1 when $\alpha = 1$.

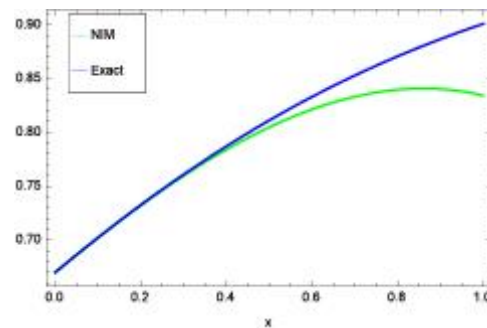


Figure 3. Comparison between approximate versus exact solution for $\alpha = 1$.

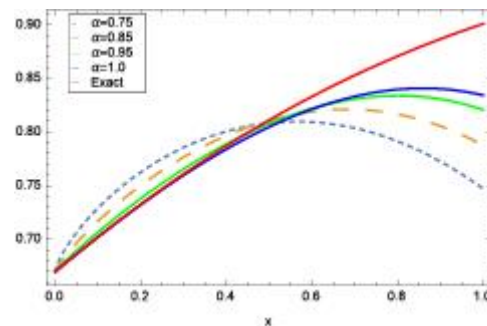


Figure 4. The numerical behavior of α on $\phi(r, \eta)$ for different values of α .

Example 2. Consider the time-fractional Cahn–Allen model given as

$$D_{\eta}^{\rho} \phi(\varepsilon, \eta) - \phi_{\varepsilon\varepsilon}(\varepsilon, \eta) + \phi^3(\varepsilon, \eta) - \phi(\varepsilon, \eta) = 0, \quad r > 0, \quad 0 < \rho \leq 1, \quad (22)$$

with initial conditions

$$\phi(\varepsilon, 0) = \frac{1}{1 + e^{\frac{\varepsilon}{\sqrt{2}}}}. \quad (23)$$

The exact solution of the above equation, when $\rho = 1$, is

$$\phi(\varepsilon, \eta) = \frac{1}{1 + \left(e^{\frac{\varepsilon}{\sqrt{2}} - \frac{3\eta}{2}} \right)}. \quad (24)$$

First, using the Elzaki transform in Equation (22), we obtain

$$E[\phi(\varepsilon, \eta)] = s^2 \left(\frac{1}{1 + e^{\frac{\varepsilon}{\sqrt{2}}}} \right) - s^\rho E[\phi_{\varepsilon\varepsilon}(\varepsilon, \eta) - \phi^3(\varepsilon, \eta) + \phi(\varepsilon, \eta)]. \quad (25)$$

Now, implementing the inverse Elzaki transform, we obtain

$$\phi(\varepsilon, \eta) = \frac{1}{1 + e^{\frac{\varepsilon}{\sqrt{2}}}} - E^{-1}[s^\rho E\{\phi_{\varepsilon\varepsilon}(\varepsilon, \eta) - \phi^3(\varepsilon, \eta) + \phi(\varepsilon, \eta)\}]. \quad (26)$$

Using the NITM, we have the following:

$$\begin{aligned} \phi_0(\varepsilon, \eta) &= \frac{1}{1 + e^{\frac{\varepsilon}{\sqrt{2}}}}, \\ \phi_1(\varepsilon, \eta) &= -E^{-1}[s^\rho E\{\phi_{0\varepsilon\varepsilon}(\varepsilon, \eta) - \phi_0^3(\varepsilon, \eta) + \phi_0(\varepsilon, \eta)\}] = \frac{3\eta^\rho}{4\rho \Gamma(\rho) + 4\rho \cosh\left(\frac{\varepsilon}{\sqrt{2}}\right) \Gamma(\rho)}, \\ \phi_2(\varepsilon, \eta) &= -E^{-1}[s^\rho E\{\phi_{1\varepsilon\varepsilon}(\varepsilon, \eta) - \phi_1^3(\varepsilon, \eta) + \phi_1(\varepsilon, \eta)\}], \\ \phi_2(\varepsilon, \eta) &= \frac{9\eta^{2\rho}}{256} \left(\frac{3\eta^\rho \left(-\frac{3\eta^\rho \Gamma(3\rho)}{(1 + \cosh^3(\frac{\varepsilon}{\sqrt{2}})) \Gamma(4\rho)} - \frac{64e^{\sqrt{2}\varepsilon} \Gamma(1+\rho) \Gamma(1+2\rho)}{\left(1 + e^{\frac{\varepsilon}{\sqrt{2}}}\right)^5 \Gamma(1+3\rho)} \right)}{\Gamma(1+3\rho)^3} - \frac{16 \operatorname{sech}^2\left(\frac{\varepsilon}{2\sqrt{2}}\right) \tanh\left(\frac{\varepsilon}{2\sqrt{2}}\right)}{\Gamma(1+2\rho)} \right), \\ &\vdots \end{aligned}$$

The series form solution is defined as

$$\phi(\varepsilon, \eta) = \phi_0(\varepsilon, \eta) + \phi_1(\varepsilon, \eta) + \phi_2(\varepsilon, \eta) + \phi_3(\varepsilon, \eta) + \dots + \phi_n(\varepsilon, \eta). \quad (27)$$

The analytical result is obtained as

$$\begin{aligned} \phi(\varepsilon, \eta) &= \frac{9\eta^{2\rho}}{256} + \frac{3\eta^\rho}{4\rho \Gamma(\rho) \cosh\left(\frac{\varepsilon}{\sqrt{2}}\right) + 4\rho \Gamma(a)} + \frac{1}{e^{\frac{\varepsilon}{\sqrt{2}}} + 1} \\ &\quad \frac{3\eta^a \left(-\frac{3\eta^\rho \Gamma(3\rho)}{\Gamma(4\rho) \left(\cosh\left(\frac{\varepsilon}{\sqrt{2}}\right) + 1\right)^3} - \frac{64e^{\sqrt{2}\varepsilon} \Gamma(\rho+1) \Gamma(2\rho+1)}{\left(e^{\frac{\varepsilon}{\sqrt{2}}} + 1\right)^5 \Gamma(3\rho+1)} \right)}{\Gamma(\rho+1)^3} + \frac{16 \tanh\left(\frac{\varepsilon}{2\sqrt{2}}\right) \operatorname{sech}^2\left(\frac{\varepsilon}{2\sqrt{2}}\right)}{\Gamma(2\rho+1)} + \dots \end{aligned} \quad (28)$$

Solution for $\rho = 1$

$$\begin{aligned} \phi(\varepsilon, \eta) &= \frac{1}{e^{\frac{\varepsilon}{\sqrt{2}}} + 1} + \frac{3\eta}{4 \cosh\left(\frac{\varepsilon}{\sqrt{2}}\right) + 4} + \frac{9}{256} \eta^2 \left(3\eta \left(-\frac{\eta}{\left(\cosh\left(\frac{\varepsilon}{\sqrt{2}}\right) + 1\right)^3} - \frac{64e^{\sqrt{2}\varepsilon}}{3\left(e^{\frac{\varepsilon}{\sqrt{2}}} + 1\right)^5} \right) \right. \\ &\quad \left. + 8 \tanh\left(\frac{\varepsilon}{2\sqrt{2}}\right) \operatorname{sech}^2\left(\frac{\varepsilon}{2\sqrt{2}}\right) \right). \end{aligned}$$

Solution for $\rho = 0.95$

$$\phi(\varepsilon, \eta) = \frac{1}{e^{\frac{\varepsilon}{\sqrt{2}}} + 1} + \frac{3\eta^{0.95}}{3.91952 \cosh\left(\frac{\varepsilon}{\sqrt{2}}\right) + 3.91952} + \frac{9}{256}\eta^{1.9}\left(3.18861\eta^{0.95}\right. \\ \left.- \frac{1.11801\eta^{0.95}}{\left(\cosh\left(\frac{\varepsilon}{\sqrt{2}}\right) + 1\right)^3} - \frac{22.9851e^{\sqrt{2}\varepsilon}}{\left(e^{\frac{\varepsilon}{\sqrt{2}}} + 1\right)^5}\right) + 8.75582 \tanh\left(\frac{\varepsilon}{2\sqrt{2}}\right) \operatorname{sech}^2\left(\frac{\varepsilon}{2\sqrt{2}}\right).$$

Solution for $\rho = 0.85$

$$\phi(\varepsilon, \eta) = \frac{1}{e^{\frac{\varepsilon}{\sqrt{2}}} + 1} + \frac{3\eta^{0.85}}{3.78244 \cosh\left(\frac{\varepsilon}{\sqrt{2}}\right) + 3.78244} + \frac{9}{256}\eta^{1.7}\left(3.548\eta^{0.85}\right. \\ \left.- \frac{1.38643\eta^{0.85}}{\left(\cosh\left(\frac{\varepsilon}{\sqrt{2}}\right) + 1\right)^3} - \frac{26.6087e^{\sqrt{2}\varepsilon}}{\left(e^{\frac{\varepsilon}{\sqrt{2}}} + 1\right)^5}\right) + 10.3581 \tanh\left(\frac{\varepsilon}{2\sqrt{2}}\right) \operatorname{sech}^2\left(\frac{\varepsilon}{2\sqrt{2}}\right).$$

Solution for $\rho = 0.75$

$$\phi(\varepsilon, \eta) = \frac{1}{e^{\frac{\varepsilon}{\sqrt{2}}} + 1} + \frac{3\eta^{0.75}}{3.67625 \cosh\left(\frac{\varepsilon}{\sqrt{2}}\right) + 3.67625} + \frac{9}{256}\eta^{1.5}\left(3.86444\eta^{0.75}\right. \\ \left.- \frac{1.6995\eta^{0.75}}{\left(\cosh\left(\frac{\varepsilon}{\sqrt{2}}\right) + 1\right)^3} - \frac{30.6724e^{\sqrt{2}\varepsilon}}{\left(e^{\frac{\varepsilon}{\sqrt{2}}} + 1\right)^5}\right) + 12.036 \tanh\left(\frac{\varepsilon}{2\sqrt{2}}\right) \operatorname{sech}^2\left(\frac{\varepsilon}{2\sqrt{2}}\right).$$

In Figures 5 and 6, the NITM and exact solutions of Problem 2 are represented. From the given figures, it is seen that both the actual and NITM solutions are close to each other. In Figure 7, the 2D surface obtained by the NITM versus the exact solution is shown, while in Figure 8, the NITM result of Example 2 is represented. Tables 1 and 2 show the comparison between the exact, homotopy perturbation method and new iterative transform method. From the tables, we can see that the suggested method is more accurate, and we confirm that the iterations increase the NITM results so that they become closer to the actual solution.

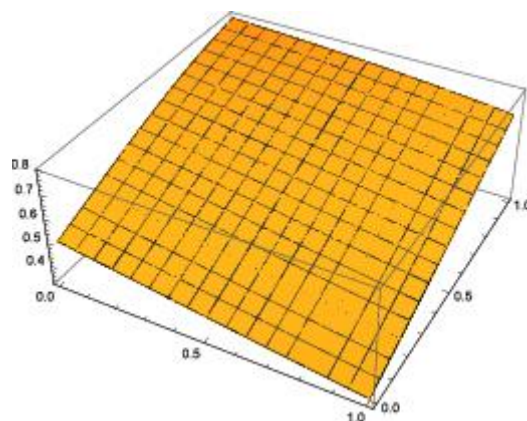


Figure 5. Approximate solution obtained by NITM for fractional-order Problem 2 when $\alpha = 1$.

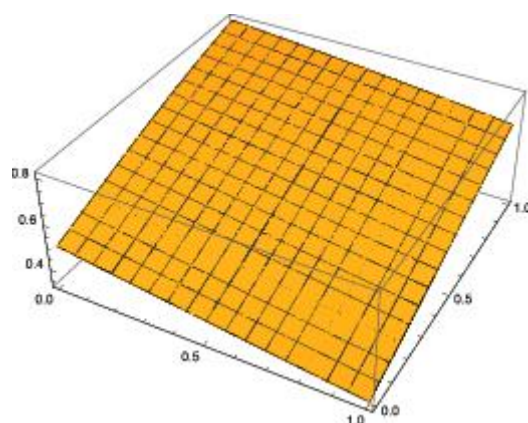


Figure 6. Exact solution graph of Problem 1 when $\alpha = 1$.

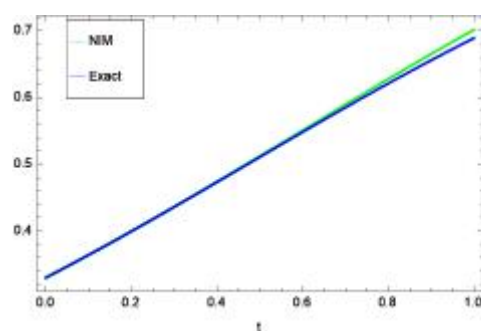


Figure 7. Comparison between approximate versus exact solution for $\alpha = 1$.

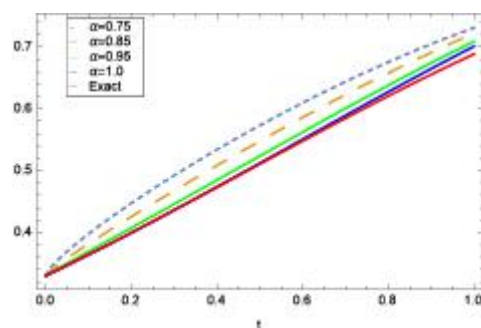


Figure 8. The numerical behavior of α on $\phi(r, \eta)$ for different values of α .

Table 1. Absolute errors obtained by NITM in comparison with HPM for Example 1, when $\rho = 1.0$.

η	ϕ	$\phi(\varepsilon, \eta)$	Exact	HPM	NITM
0.001	1	0.670093	0.670093	1.0×10^{-6}	3.3×10^{-11}
0.002	1	0.670425	0.670425	1.0×10^{-5}	2.6×10^{-10}
0.003	1	0.670756	0.670756	9.0×10^{-5}	8.9×10^{-10}
0.004	1	0.671087	0.671087	2.5×10^{-6}	2.1×10^{-9}
0.005	1	0.671418	0.671418	4.7×10^{-6}	4.1×10^{-9}
0.006	1	0.671749	0.671749	8.6×10^{-6}	7.1×10^{-9}
0.007	1	0.67208	0.67208	1.3×10^{-6}	1.1×10^{-8}
0.008	1	0.67241	0.67241	2.0×10^{-6}	1.7×10^{-8}
0.009	1	0.672741	0.672741	2.9×10^{-6}	2.4×10^{-8}
0.01	1	0.673071	0.673071	4.0×10^{-6}	3.3×10^{-8}

Table 2. Absolute errors obtained by NITM in comparison with HPM, when $\rho = 1.0$.

η	ϕ	$u(\varepsilon, \eta)$	Exact	HPM	NITM
0.001	1	0.33057	0.33057	7.6×10^{-12}	4.3×10^{-12}
0.002	1	0.330902	0.330902	3.8×10^{-10}	3.5×10^{-11}
0.003	1	0.331235	0.331235	1.1×10^{-9}	1.1×10^{-10}
0.004	1	0.331567	0.331567	2.6×10^{-9}	2.8×10^{-10}
0.005	1	0.331899	0.331899	5.0×10^{-9}	5.5×10^{-10}
0.006	1	0.332232	0.332232	9.7×10^{-9}	9.6×10^{-10}
0.007	1	0.332565	0.332565	1.5×10^{-8}	1.5×10^{-9}
0.008	1	0.332898	0.332898	2.0×10^{-8}	2.2×10^{-9}
0.009	1	0.333231	0.333231	2.9×10^{-8}	2.3×10^{-9}
0.01	1	0.333565	0.333565	4.0×10^{-8}	4.5×10^{-9}

5. Conclusions

In the current work, a novel method known as the new iterative transform method obtains the series solution of the fractional-order Cahn–Allen equation. The acquired solution by the current strategy was checked through different graphs and numerical simulations. We found that there exists an excellent mutual understanding between the derived and actual results of the problems. From the above conversation, it is demonstrated that the current technique is more sensible and quickly convergent to the actual results of the targeted problems.

Author Contributions: Conceptualization, L.A and R.S.; methodology, R.S.; software, W.W.; validation, L.A., R.S. and W.W.; formal analysis, W.W.; investigation, L.A.; resources, W.W.; data curation, R.S.; writing—original draft preparation, R.S.; writing—review and editing, L.A.; visualization, W.W.; supervision, W.W.; project administration, R.S.; funding acquisition, W.W. All authors have read and agreed to the published version of the manuscript.

Funding: This research received funding support from the NSRF via the Program Management Unit for Human Resources & Institutional Development, Research and Innovation (grant number B05F640092).

Institutional Review Board Statement: Not applicable.

Informed Consent Statement: Not applicable.

Data Availability Statement: The numerical data used to support the findings of this study are included within the article.

Conflicts of Interest: The authors declare that there are no conflict of interest regarding the publication of this article.

References

1. Baleanu, D.; Guevenc, Z.B.; Machado, J.T. (Eds.) *New Trends in Nanotechnology and Fractional Calculus Applications*; Springer: New York, NY, USA, 2010; p. C397.
2. Caponetto, R. *Fractional Order Systems: Modeling and Control Applications*; World Scientific: Singapore, 2010; Volume 72.
3. Diethelm, K. *The Analysis of Fractional Differential Equations: An Application-Oriented Exposition Using Differential Operators of Caputo Type*; Springer Science & Business Media: Berlin/Heidelberg, Germany, 2010.
4. Hilfer, R. (Ed.) *Applications of Fractional Calculus in Physics*; World Scientific: Singapore, 2000.
5. Wazwaz, A.M. *First Course In Integral Equations, A*; World Scientific Publishing Company: Singapore, 2015.
6. Shah, R.; Khan, H.; Baleanu, D.; Kumam, P.; Arif, M. A novel method for the analytical solution of fractional Zakharov-Kuznetsov equations. *Adv. Differ. Equ.* **2019**, *2019*, 517.
7. Kilbas, A.A.; Srivastava, H.M.; Trujillo, J.J. *Theory and Applications of Fractional Differential Equations*; Elsevier: Amsterdam, The Netherlands, 2006; Volume 204.
8. Helal, M.A.; Mehanna, M.S. A comparative study between two different methods for solving the general Korteweg-de Vries equation (GKdV). *Chaos Solitons Fractals* **2007**, *33*, 725–739.
9. Jibran, M.; Nawaz, R.; Khan, A.; Afzal, S. Iterative solutions of Hirota Satsuma coupled KDV and modified coupled KDV systems. *Math. Probl. Eng.* **2018**, *2018*, 9042039.

10. Yasar, E.; Giresunlu, I.B. The $(G'/G, 1/G)$ -expansion method for solving nonlinear space-time fractional differential equations. *Pramana* **2016**, *87*, 17.
11. Esen, A.L.A.A.T.T.I.N.; Yagmurlu, N.M.; Tasbozan, O. Approximate analytical solution to time-fractional damped Burger and Cahn-Allen equations. *Appl. Math. Inf. Sci.* **2013**, *7*, 1951.
12. Jafari, H.; Tajadodi, H.; Baleanu, D. Application of a homogeneous balance method to exact solutions of nonlinear fractional evolution equations. *J. Comput. Nonlinear Dyn.* **2014**, *9*, 021019-1.
13. Hariharan, G.; Kannan, K. Haar wavelet method for solving Cahn-Allen equation. *Appl. Math. Sci.* **2009**, *3*, 2523–2533.
14. Tascan, F.; Bekir, A. Travelling wave solutions of the Cahn-Allen equation by using first integral method. *Appl. Math. Comput.* **2009**, *207*, 279–282.
15. Tariq, H.; Akram, G. New traveling wave exact and approximate solutions for the nonlinear Cahn-Allen equation: Evolution of a nonconserved quantity. *Nonlinear Dyn.* **2017**, *88*, 581–594.
16. Bekir, A. Multisoliton solutions to Cahn-Allen equation using double exp-function method. *Phys. Wave Phenom.* **2012**, *20*, 118–121.
17. Guner, O.; Bekir, A.; Cevikel, A.C. A variety of exact solutions for the time fractional Cahn-Allen equation. *Eur. Phys. J. Plus* **2015**, *130*, 1–13.
18. Daftardar-Gejji, V.; Jafari, H. An iterative method for solving nonlinear functional equations. *J. Math. Anal. Appl.* **2006**, *316*, 753–763.
19. Jafari, H. Iterative Methods for Solving System of Fractional Differential Equations. Ph.D. Thesis, Pune University, Pune, India, 2006.
20. Jafari, H.; Nazari, M.; Baleanu, D.; Khalique, C.M. A new approach for solving a system of fractional partial differential equations. *Comput. Math. Appl.* **2013**, *66*, 838–843.
21. Ramadan, M.A.; Al-luhaibi, M.S. New iterative method for solving the fornberg-whitham equation and comparison with homotopy perturbation transform method. *J. Adv. Math. Comput. Sci.* **2014**, *4*, 1213–1227.
22. Prakash, A.; Kumar, M.; Baleanu, D. A new iterative technique for a fractional model of nonlinear Zakharov-Kuznetsov equations via Sumudu transform. *Appl. Math. Comput.* **2018**, *334*, 30–40.
23. Yan, L. Numerical solutions of fractional Fokker-Planck equations using iterative Laplace transform method. In *Abstract and Applied Analysis*; Hindawi: London, UK, 2013; Volume 2013.
24. Elzaki, T.M. The new integral transform Elzaki transform. *Glob. J. Pure Appl. Math.* **2011**, *7*, 57–64.
25. Alshikh, A.A.; Mahgob, M.M.A. A comparative study between Laplace transform and two new integrals “Elzaki” transform and “Aboodh” transform. *Pure Appl. Math. J.* **2016**, *5*, 145–150.
26. Elzaki, T.M.; Alkhateeb, S.A. Modification of Sumudu transform “Elzaki transform” and Adomian decomposition method. *Appl. Math. Sci.* **2015**, *9*, 603–611.